Journal of Nuclear Medicine, published on April 7, 2022 as doi:10.2967/jnumed.121.263707

Validation of ^{18}F-rhPSMA-7 and ^{18}F-rhPSMA-7.3 PET imaging results with histopathology from salvage surgery in patients with biochemical recurrence of prostate cancer

Markus Kroenke[1,2], Lilit Schweiger[1,3], Thomas Horn[4], Bernhard Haller[5], Kristina Schwamborn[6], Alexander Wurzer[1,7], Tobias Maurer[8], Hans-Jürgen Wester[7], Matthias Eiber[1,3*], Isabel Rauscher[1,3*]

*contributed equally

[1] Department of Nuclear Medicine, School of Medicine, Technical University of Munich, Germany
[2] Department of Radiology and Nuclear Medicine, German Heart Center Munich, Technical University of Munich, Munich, Germany
[3] Bavarian Cancer Research Center (BZKF)
[4] Department of Urology, School of Medicine, Technical University of Munich, Germany
[5] Institute of Medical Informatics, Statistics and Epidemiology, School of Medicine, Technical University of Munich, Germany
[6] Department of Pathology, School of Medicine, Technical University of Munich, Germany
[7] Chair of Radiopharmacy, School of Medicine, Technical University of Munich, Germany
[8] Martini-Klinik and Department of Urology, University Hospital Hamburg-Eppendorf, Germany

First author:
Dr. med Markus Kroenke
Department of Radiology and Nuclear Medicine
German Heart Center Munich,
Lazarettstr. 36, 80636 Munich, Germany
Phone +49 (0)89 1218 4547
Fax +49 (0)89 1218 4513
E-mail kroenke@dhm.mhn.de

Corresponding author:
PD Dr. med. Isabel Rauscher
Department of Nuclear Medicine
School of Medicine, Technical University of Munich
Ismaninger Str. 22, 81675 Munich, Germany
Phone +49 (0)89 4140 2972
Fax +49 (0)89 4140 4950
Email isabel.rauscher@tum.de

Word count: 5644
Running title: Histopathological validation of F-rhPSMA PET

Keywords: ^{18}F-rhPSMA-7, ^{18}F-rhPSMA-7.3, prostate cancer, salvage surgery, biochemical recurrence, prostate-specific membrane antigen

Conflict of Interests: Patent application for rhPSMA (HJW, AW and ME). HJW and ME received funding Blue Earth Diagnostics Ltd (Oxford, UK, Licensee for rhPSMA) as part of an academic collaboration. ME reports prior consulting activities for Blue Earth Diagnostics Ltd., Novartis, Telix, Progenics, Bayer, Point Biopharma and Janssen. HJW is founder, shareholder and advisor board member of Scintomics GmbH (Fuerstenfeldbruck, Germany). Siemens Medical Solutions (Erlangen, Germany) supported the application of Biograph mCT flow as part of an academic collaboration. TM reports prior consulting activities for Blue Earth Diagnostics Ltd., Novartis, Telix, ROTOP Pharma, Advanced Accelerator Applications International S.A., GEMoAb and Astellas.
No other potential conflicts of interest relevant to this article exist.

ABSTRACT

^{18}F-rhPSMA-7, and its single diastereoisomer form, ^{18}F-rhPSMA-7.3, are novel prostate specific membrane antigen (PSMA)-targeting radiopharmaceuticals. Here, we investigated their accuracy for the assessment of lymph node metastases validated by histopathology. **Methods:** Data from 58 patients with biochemical recurrence of prostate cancer after radical prostatectomy receiving salvage surgery after positron emission tomography (PET) imaging with ^{18}F-rhPSMA-7 or ^{18}F-rhPSMA-7.3 were retrospectively reviewed. Two nuclear medicine physicians reviewed all PET scans and morphological imaging in consensus. Readers were blinded from the results of histopathology. PET and morphological imaging were correlated with histopathology from resected lymph nodes. **Results:** In 75 of 150 resected regions in 54 of 58 patients, tumor lesions were present in histopathology. The template-based specificity of PET (^{18}F-rhPSMA-7 and ^{18}F-rhPSMA-7.3 combined) and morphologic imaging were 93.3% and 100%, respectively. However, ^{18}F-rhPSMA-7 and ^{18}F-rhPSMA-7.3 PET detected metastases in 61 of 75 histopathologically proven metastatic LN fields (81.3%) whereas morphologic imaging was positive in only 9 of 75 (12.0%). The positive predictive value for ^{18}F-rhPSMA-7 and ^{18}F-rhPSMA-7.3 PET was 92.4% vs 100% for morphological imaging. ^{18}F-rhPSMA-7 and ^{18}F-rhPSMA-7.3 PET performance was significantly superior to morphological imaging (difference in the areas under the receiver-operating-characteristic curves, 0.222; 95% confidence interval, 0.147-0.298; $p<0.001$). Mean size of PET-positive and histologically confirmed LN metastases was 6.3±3.1 mm (range, 2-15 mm) compared to a mean size of 9.8 ± 2.5 mm (range, 7-15 mm) in morphological imaging. **Conclusion:** ^{18}F-rhPSMA-7 and ^{18}F-rhPSMA-7.3 PET offer a high positive predictive value comparable to that reported for ^{68}Ga-PSMA-11 and represent a valuable tool for guiding salvage lymphadenectomy.

INTRODUCTION

Up to one third of all patients with prostate cancer (PC) will experience biochemical recurrence after initial curative-intended treatment (*1*). Salvage therapies such as salvage surgery and other metastasis-directed treatments can prolong the interval until systemic therapy is needed (*2-4*). To perform any localized treatment, for either metastasis or local recurrence, accurate diagnostic imaging is of utmost importance. Several studies have already proven the superiority of positron emission tomography (PET) targeting the prostate-specific membrane antigen (PSMA) compared with morphological imaging (e.g. computed tomography (CT) and magnetic resonance imaging (MRI)) for localization of recurrent disease or for primary N-staging (*5,6*). In this context, ^{68}Ga-PSMA-11 has been the PSMA-ligand most extensively assessed in several retrospective and prospective studies leading to its approval and recommendation by various guidelines as the preferred imaging tool for restaging (*7-11*).

However, ^{18}F-labelled PSMA-targeting ligands are becoming increasingly used in preference to ^{68}Ga-labelled counterparts due to the principal advantages of radiofluorinated tracers (e.g. longer half-life and large batch production in cyclotrons leading to the possibility of centralized production and distribution as well as lower positron energy of ^{18}F compared with ^{68}Ga)(*12*).

^{18}F-rhPSMA-7 is one such ^{18}F-labelled PSMA-targeting ligand representing a class of radiohybrid PSMA (rhPSMA) ligands which can be labelled with ^{18}F for imaging purposes, but also with other radioactive isotopes such as ^{177}Lutetium for endoradiotherapy (*13*). ^{18}F-rhPSMA-7 is composed of four diastereoisomers (^{18}F-rhPSMA-7.1-7.4) (*14*). Of these, ^{18}F-rhPSMA-7.3 was selected for clinical development based on its superior characteristics in preclinical studies,

including fast clearance from blood pool, liver and kidneys as well as high tumor accumulation in LNCaP tumor-bearing mice (*14*). It is currently under investigation in two multicenter phase III trials for PET imaging (NCT04186845 and NCT04186819). ^{18}F-rhPSMA-7.3 shows very similar properties as the isomeric mixture ^{18}F-rhPSMA-7 with both PSMA-ligands showing high detection rates in patients with biochemical recurrence of PC (*15,16*).

However, to date, no histopathological validated study has been published on the utilization in patients with biochemical recurrence of PC. Thus, the aim of this retrospective analysis was to assess the performance of ^{18}F-rhPSMA-7 and ^{18}F-rhPSMA-7.3 PET in patients with biochemical recurrence after radical prostatectomy undergoing subsequent salvage surgery for histopathological comparison.

METHODS

Patients

We retrospectively reviewed the institution´s database for all patients with biochemical recurrence of PC who underwent either ^{18}F-rhPSMA-7 or ^{18}F-rhPSMA-7.3 PET and subsequent salvage surgery between November 2017 and June 2020. Patients were excluded if they had not undergone radical prostatectomy as a primary treatment. In total, 58 patients were identified. The retrospective analysis was approved by the local Ethics Committee (permit 290/18S and 99/19). Administration of ^{18}F-rhPSMA-7 and ^{18}F-rhPSMA-7.3 complied with the German Medicinal Products Act, AMG §13 2b, and the responsible regulatory body (government of Oberbayern).

^{18}F-rhPSMA Synthesis, Administration, and PET Imaging

^{18}F-rhPSMA-7 and ^{18}F-rhPSMA-7.3 were synthesized and utilized as reported previously (*13,17,18*). Twenty-three (40%) patients received ^{18}F-rhPSMA-7 and 35 (60%) patients received the single-isomer ^{18}F-rhPSMA-7.3. ^{18}F-rhPSMA-7 and ^{18}F-rhPSMA-7.3 were administered (median activity 320 MBq; range 239-399 MBq) as an intravenous bolus a median of 72 min (range, 60-148 min) before scanning. In total, 49 patients underwent contrast-enhanced PET/CT (Biograph mCT Flow; Siemens Healthineers, Erlangen, Germany; contrast agent: Imeron 300; Bracco Imaging, Konstanz, Germany) and 9 patients underwent PET/MRI (Biograph mMR; Siemens Healthineers, Erlangen, Germany). The fully diagnostic PET/CT and PET/MRI examinations were conducted as previously reported (*19,20*). Furosemide (20 mg i.v.) was administered to all patients at the time of tracer application and patients were asked to void urine prior to the scan.

All PET/CT scans were acquired in 3-dimensional mode with time of flight and in continuous table motion (flowMotion technology, Siemens (*21*) with 1.1 mm/s, equal to 2 min per bed position. The PET/MRI scans were acquired in 3-dimensional mode and step-and-shoot with 4 min per bed position for PET/MRI. Emission data were corrected for randoms, dead time, scatter, and attenuation and were reconstructed iteratively by an ordered-subsets expectation maximization algorithm (4 iterations, 8 subsets) followed by a post-reconstruction smoothing gaussian filter (5 mm in full width at half maximum).

Image Analysis

All ^{18}F-rhPSMA-7 and ^{18}F-rhPSMA-7.3 PET/CT and PET/MRI datasets were reviewed by 2 experienced board-certified nuclear medicine specialists in consensus. The readers were blinded to the results of histopathology. First, the CT dataset of the PET/CT or the dedicated high resolution axial T2-weighted TSE sequence of the pelvis up to the aortic bifurcation (slice

thickness 5 mm each) of the PET/MRI were analyzed. Second, after a time interval of at least 4 weeks, the corresponding ^{18}F-rhPSMA-7 and ^{18}F-rhPSMA-7.3 PET scans were read by the same readers, with the morphological imaging only being used for anatomic allocation. Findings were rated using a 5-point Likert scale as described in (*22*): PET rating of 5 indicates a tumor manifestation (intense, focal uptake, uptake higher than in the liver); 4, probable tumor manifestation (uptake clearly higher than the background level in vessels but less than in the liver); 3, equivocal findings (faint uptake between muscle and vessels uptake); 2, probable benign findings (uptake equal to the adjacent muscle); 1, benign findings (no uptake).

For both CT and MRI, the same Likert scale was applied with a rating of 5 indicating tumor manifestation (lymph node short-axis diameter >10mm); 4, probable tumor manifestation (short-axis diameter of 8-10 mm and/or a round configuration and/or a regional grouping); 3, equivocal findings (short-axis diameter of 8-10 mm, an oval configuration, and no regional grouping); 2, probable benign findings (short-axis diameter <8 mm); and 1, benign findings (short-axis diameter < 5mm). Finally, SUVmax and size (short-axis diameter) of the largest lymph node per template region rated with score 4 or 5 was measured.

Surgery and Histopathology

The patients were selected for salvage surgery by an inter-disciplinary tumor board based on clinical characteristics and the initial clinical reads of ^{18}F-rhPSMA-7 or ^{18}F-rhPSMA-7.3 PET. The salvage surgery was planned based on the information on PET and the surgical fields were limited to the pelvis including potential local recurrence. Depending on the location, adjacent lymph node template regions were resected as well. The lymph node template regions were separately collected. Uro-pathologists were blinded to imaging results.

Statistical Analysis

The histopathologic results from resected lymph nodes were correlated with the results of morphological imaging (MRI or CT) and ^{18}F-rhPSMA-7/ 7.3 PET in a patient- and template-based manner. Further a separate template-based analysis of ^{18}F-rhPSMA-7 and ^{18}F-rhPSMA-7.3 was performed. Results from the 5-point Likert scale were dichotomized to allow estimation of sensitivity, specificity, positive predictive value, and accuracy. For the statistical analysis, we decided that only scores indicating definitive or probable tumor manifestation in PET and morphological imaging (scores ≥4) were counted as positive for statistical analysis. This was based on clinical consideration that invasive procedures (e.g. secondary lymphadenectomy and associated general anesthesia) with its potential risks are not justified if only equivocal findings (score 3) were present.

The overall diagnostic accuracy of template-based data was assessed using receiver-operating-characteristic (ROC) analyses. ROC curves were calculated for both modalities. Areas under the ROC curves with 95% confidence intervals (CI) were calculated and compared with each other. The approach proposed by Obuchowski was considered for region-based analyses to account for correlations of multiple findings within one patient with the help of generalized estimating equations extension of linear regression model (*23*). A significance level of 5% was considered for all tests. All statistical analyses were performed using the statistical software R with its packages pROC and geepack (*24-26*).

RESULTS

Patient Characteristics and Histopathologic Results

Data of 58 patients was reviewed. The patients presented with a median age of 68.5 years (range 51-85) and a median prostate specific antigen (PSA) level of 0.71 ng/mL (range 0.16-8.39) prior to the PET scan. Detailed patient characteristics are presented in Table 1. Supplemental Tables 1 and 2 provide detailed per-patient information on patient characteristics, imaging methods and results.

In 54 of 58 patients, pelvic tumor lesions were confirmed by histopathology. Overall, 150 template regions were resected with 75 of them harboring tumor lesions (50%). Most (n=129) were part of the typical pelvic lymph node template. Other resected regions were 9 retroperitoneal locations (n=6 positive on histopathology) and 12 local regions due to suspicion of local recurrence (n=10 positive on histopathology).

Imaging Results

Template-based Area under the ROC curve for ^{18}F-rhPSMA-7/7.3 was 0.891 (95% CI, 0.838–0.944) and for morphologic imaging 0.669 (95% CI, 0.595–0.742, Fig. 1). ^{18}F-rhPSMA-7/7.3 PET performed significantly better than morphologic imaging for the detection of lymph node metastases (difference in Areas under the ROC curves, 0.222; 95% CI, 0.147-0.298; $p<0.001$).

On the template-based analysis, specificity was 93.3% (95% CI, 85.9-97.0%) and 100% (95% CI, n/a) for ^{18}F-rhPSMA-7/7.3 PET and morphologic imaging, respectively. ^{18}F-rhPSMA-7/7.3 PET detected lymph node metastases in 61 of 75 histopathologically proven metastatic lymph node template regions (sensitivity, 81.3%; 95% CI, 70.1-89.0%) whereas morphologic imaging was

positive in only 9 of 75 lymph node templates (sensitivity, 12.0% 95% CI, 6.3-21.6%). The positive predictive value was 92.4% for ^{18}F-rhPSMA-7/7.3 PET and 100% for morphologic imaging. Diagnostic accuracy of ^{18}F-rhPSMA-7/ 7.3 PET was 87.3% (95% CI, 80.5-92.0%) and 64.5% (95% CI, 47.2-64.5%) for morphologic imaging, respectively (Table 2).

In detail, 75 template regions were free of tumor invasion after histopathologic evaluation, with 70 of them being correctly identified as negative with PET and 75 of them being correctly identified as negative with morphologic imaging. Five template regions (in 3 patients) were classified as suspicious in PET with no correlation in histopathology (false positive), while morphologic imaging resulted in no template regions being judged as false positive. Follow-up was available in two of the false-positive patients in PET with slightly increasing PSA-levels after surgery but no sign of metastasis in the follow-up ^{18}F-rhPSMA-7/ 7.3 PET scan.

Fourteen template regions were false negative in PET, whereas in morphologic imaging, 66 template regions resulted in a false negative finding. Data for the patient-based analysis is presented in Supplemental Table 3. A separate analysis of ^{18}F-rhPSMA-7 and ^{18}F-rhPSMA-7.3 is presented in Supplemental Table 4. Here, ^{18}F-rhPSMA-7 and ^{18}F-rhPSMA-7.3 PET presented with a similar PPV (92.3 for ^{18}F-rhPSMA-7 and 92.5% for ^{18}F-rhPSMA-7.3, respectively).

Uptake in ^{18}F-rhPSMA-7 and ^{18}F-rhPSMA-7.3 PET and Lesion Size

The mean SUVmax of histologically confirmed pelvic lymph node metastases rated suspicious in PET was 16.7±24.7 (range, 3.3-146.6). The corresponding mean lesion size of these PET-positive, histologically confirmed lymph nodes was 6.3±3.1 mm (range, 2-15 mm). The mean size of histologically confirmed lymph nodes rated as suspicious on morphological imaging was

10.6±2.7 mm (range, 7-15 mm). The mean size of histologically confirmed lymph nodes not rated as suspicious on morphological imaging was 5.3±2.3 mm (range, 2-14 mm).

A representative example of a correctly classified lymph node metastases by PET/CT is shown in Figure 2.

DISCUSSION

The value of PSMA PET for imaging patients with recurrence of PC after primary treatment has been extensively reported (*5,6,20,27-29*). Here, we reviewed real-world clinical data supporting the utility of the novel PSMA-targeting radiopharmaceuticals ^{18}F-rhPSMA-7/7.3. To date, the efficacy of both ^{18}F-rhPSMA-7 and ^{18}F-rhPSMA-7.3 for imaging PC patients have been demonstrated by several retrospective studies (*15,16,30*), including their high accuracy for lymph node staging in patients with primary PC (*22,31*). The presented data demonstrate a high specificity and positive predictive value of ^{18}F-rhPSMA-7/7.3 PET for lymph node metastases in patients with recurrent PC after radical prostatectomy validated by histopathology. On a template-based analysis it offers a higher accuracy and sensitivity compared with morphological imaging.

These results are in line with a similar, histopathologically validated analysis with ^{68}Ga-PSMA-11 showing a sensitivity, specificity, positive predictive value of 77.9%, 97.3% and 94.6% compared to 81.3%, 93.3% and 92.4% in our analysis, respectively (*5*). Further, the difference in the areas under the receiver-operating-characteristic curves to morphologic images were 0.139 with ^{68}Ga-PSMA-11 compared to 0.222 with ^{18}F-rhPSMA-7/7.3 in our analysis (*5*). Similar to ^{68}Ga-PSMA-11 PET, our data show that these novel tracers can detect small lymph node metastasis with a lesion size smaller than 10 mm in the recurrent PC setting (*5*). Salvage lymph node surgery

represents a therapeutic option for patients experiencing biochemical recurrence after radical prostatectomy and previous ^{11}C-choline PET-guided data suggest that up to 40% of patients may experience recurrence-free survival following PET-guided salvage lymph node dissection (*32*). More recently, Horn et al. showed that in a subgroup of patients with recurrent PC undergoing PSMA PET-guided salvage surgery, complete biochemical response was achieved in 66% of patients (*2*). Moreover, it is believed that PET-guided salvage lymph node dissection may prolong the time until initiation of hormonal treatment, which is associated with significant morbidity, is needed (*33,34*). For salvage surgery with potential complications a high specificity and positive predictive value is of utmost importance to avoid unnecessary interventions. Interestingly, specificity of morphological imaging on a template base was also excellent which is most likely related to the strict criteria for the determination of metastases. However, as known from the literature, its sensitivity is rather low as it can only detect lymph node metastases with already enlarged (>10 mm) lesions.

The pure enantiomeric form of ^{18}F-rhPSMA-7, ^{18}F-rhPSMA-7.3, has been selected as the lead rhPSMA compound for clinical development based on preclinical assessments showing favorable safety and kinetic profiles for diagnostic imaging of PC (*14,18*). Due to the limited numbers, no sound comparison of the diagnostic performance of ^{18}F-rhPSMA-7 vs. ^{18}F-rhPSMA-7.3 is possible in the present study. However, we note similar positive predictive values for the two compounds, which is the only descriptive statistical value to be unaffected by the potential selection bias that results from the present study design. Another limitation of this retrospective analysis is its potential selection bias. This is induced due to the selection of patients and the lymph node template regions to be removed based on the clinical reads of the ^{18}F-rhPSMA-7 and

^{18}F-rhPSMA-7.3 PET scan. Possible imaging-negative nodes could have been missed, which would impact the sensitivity estimate. Therefore, PPV is the only descriptive statistical value independent of this bias. Of note, specificity on the patient-based analysis was only informed by 4 cases (Supplemental Table 3). Due to different reasons, it was not always feasible to perform surgery shortly after PET examination (median time between PET and surgery of 59 days; range 19-117 days), respectively. Thus, in principle it cannot be excluded that there was tumor progression or even new tumor lesions at time of surgery. The data presented in the supplementals for separate analyses of ^{18}F-rhPSMA-7 and ^{18}F-rhPSMA-7.3 should be interpreted with caution given the limited number of patients in each group. Further prospective studies with ^{18}F-rhPSMA-7.3 are warranted to confirm the diagnostic accuracy for lymph node staging and to avoid potential bias. Finally, it was not always feasible to perform surgery in a timely manner after PET.

CONCLUSION

^{18}F-rhPSMA-7 and ^{18}F-rhPSMA-7.3 PET are superior to morphological imaging for detecting pelvic lymph node metastases and helping guide salvage lymph node surgery. They offer a high positive predictive value, comparable to that reported for ^{68}Ga-PSMA-11, while yielding the benefits of a radiofluorinated tracer such as the potential for scale production and wide-range distribution.

KEY POINTS

QUESTION: What is the value of the radiopharmaceutical ^{18}F-rhPSMA-7/7.3 for assessing the presence of lymph node metastases prior to potential salvage lymphadenectomy?

PERTINENT FINDINGS: This histopathological validated, retrospective study shows that ^{18}F-rhPSMA-7/7.3 is superior to morphological imaging and comparable to ^{68}Ga-PSMA-11 for N-staging of biochemical recurrent prostate cancer.

IMPLICATIONS FOR PATIENT CARE: ^{18}F-rhPSMA-7/7.3 can detect small soft tissue metastases with a high, template-based specificity of 93%.

REFERENCES

1. Freedland SJ, Presti JC, Jr., Amling CL, et al. Time trends in biochemical recurrence after radical prostatectomy: results of the SEARCH database. *Urology.* 2003;61:736–741.

2. Horn T, Kroenke M, Rauscher I, et al. Single lesion on prostate-specific membrane antigen-ligand positron emission tomography and low prostate-specific antigen are prognostic factors for a favorable biochemical response to prostate-specific membrane antigen-targeted radioguided surgery in recurrent prostate cancer. *Eur Urol.* 2019;76:517–523.

3. Bandini M, Fossati N, Briganti A. Salvage surgery for nodal recurrent prostate cancer. *Curr Opin Urol.* 2017;27:604–611.

4. Steuber T, Jilg C, Tennstedt P, et al. Standard of care versus metastases-directed therapy for PET-detected nodal oligorecurrent prostate cancer following multimodality treatment: a multi-institutional case-control study. *Eur Urol Focus.* 2019;5:1007–1013.

5. Rauscher I, Maurer T, Beer AJ, et al. Value of ^{68}Ga-PSMA HBED-CC PET for the assessment of lymph node metastases in prostate cancer patients with biochemical recurrence: comparison with histopathology after salvage lymphadenectomy. *J Nucl Med.* 2016;57:1713–1719.

6. Maurer T, Gschwend JE, Rauscher I, et al. Diagnostic efficacy of ^{68}Gallium-PSMA positron emission tomography compared to conventional imaging for lymph node staging of 130 consecutive patients with intermediate to high risk prostate cancer. *J Urol.* 2016;195:1436–1443.

7. Eder M, Schafer M, Bauder-Wust U, et al. ^{68}Ga-complex lipophilicity and the targeting property of a urea-based PSMA inhibitor for PET imaging. *Bioconjug Chem.* 2012;23:688–697.

8. Afshar-Oromieh A, Malcher A, Eder M, et al. PET imaging with a [^{68}Ga]gallium-labelled PSMA ligand for the diagnosis of prostate cancer: biodistribution in humans and first evaluation of tumour lesions. *Eur J Nucl Med Mol Imaging.* 2013;40:486-495.

9. Perera M, Papa N, Christidis D, et al. Sensitivity, specificity, and predictors of positive ^{68}Ga-prostate-specific membrane antigen positron emission tomography in advanced prostate cancer: A systematic review and meta-analysis. *Eur Urol.* 2016;70:926–937.

10. Cornford P, Bellmunt J, Bolla M, et al. EAU-ESTRO-SIOG guidelines on prostate cancer. Part II: Treatment of relapsing, metastatic, and castration-resistant prostate cancer. *Eur Urol.* 2017;71:630-642.

11. Fendler WP. Assessment of ^{68}Ga-PSMA-11 PET accuracy in localizing recurrent prostate cancer: A prospective single-arm clinical trial. *JAMA Oncology.* 2019;5:856–863.

12. Oh SW, Wurzer A, Teoh EJ, et al. Quantitative and qualitative analyses of biodistribution and PET image quality of novel radiohybrid PSMA, ^{18}F- rhPSMA-7, in patients with prostate cancer. *J Nucl Med.* 2019;61:702–709.

13. Wurzer A, DiCarlo D, Schmidt A, et al. Radiohybrid ligands: a novel tracer concept exemplified by ^{18}F- or ^{68}Ga-labeled rhPSMA-inhibitors. *J Nucl Med.* 2019;61:735–742.

14. Wurzer A, Parzinger M, Konrad M, et al. Preclinical comparison of four [^{18}F, ^{nat}Ga]rhPSMA-7 isomers: influence of the stereoconfiguration on pharmacokinetics. *EJNMMI Research.* 2020;10:149.

15. Rauscher I, Karimzadeh A, Schiller K, et al. Detection efficacy of ^{18}F-rhPSMA-7.3 PET/CT and impact on patient management in patients with biochemical recurrence of prostate cancer after radical prostatectomy and prior to potential salvage treatment. *J Nucl Med.* 2021;62:12.

16. Eiber M, Kronke M, Wurzer A, et al. ^{18}F-rhPSMA-7 positron emission tomography for the detection of biochemical recurrence of prostate cancer following radical prostatectomy. *J Nucl Med.* 2019;61:696–701.

17. Wurzer A, Di Carlo D, Herz M, et al. Automated synthesis of [^{18}F]Ga-rhPSMA-7/ -7.3: results, quality control and experience from more than 200 routine productions. *EJNMMI Radiopharm Chem.* 2021;6:4.

18. Tolvanen T, Kalliokoski KK, Malaspina S, et al. Safety, biodistribution and radiation dosimetry of ^{18}F-rhPSMA-7.3 in healthy adult volunteers. *J Nucl Med.* 2021;62:679–684.

19. Souvatzoglou M, Eiber M, Martinez-Moeller A, et al. PET/MR in prostate cancer: technical aspects and potential diagnostic value. *Eur J Nucl Med Mol Imaging.* 2013;40 Suppl 1:S79–88.

20. Eiber M, Maurer T, Souvatzoglou M, et al. Evaluation of hybrid ^{68}Ga-PSMA ligand PET/CT in 248 patients with biochemical recurrence after radical prostatectomy. *J Nucl Med.* 2015;56:668–674.

21. Rausch I, Cal-Gonzalez J, Dapra D, et al. Performance evaluation of the Biograph mCT Flow PET/CT system according to the NEMA NU2-2012 standard. *EJNMMI Phys.* 2015;2:26.

22. Kronke M, Wurzer A, Schwamborn K, et al. Histologically-confirmed diagnostic efficacy of ^{18}F-rhPSMA-7 positron emission tomography for N-staging of patients with primary high risk prostate cancer. *J Nucl Med.* 2019;61:710–715.

23. Obuchowski NA. Nonparametric analysis of clustered ROC curve data. *Biometrics.* 1997;53:567–578.

24. The R project. The R project for statistical computing; https://www.R-project.org/. Accessed December, 2021.

25. Robin X, Turck N, Hainard A, et al. pROC: an open-source package for R and S+ to analyze and compare ROC curves. *BMC Bioinformatics.* 2011;12:77.

26. Højsgaard S, Halekoh U, Yan J. The R package geepack for generalized estimating equations. *2005.* 2005;15:11.

27. Afshar-Oromieh A, Avtzi E, Giesel FL, et al. The diagnostic value of PET/CT imaging with the ^{68}Ga-labelled PSMA ligand HBED-CC in the diagnosis of recurrent prostate cancer. *Eur J Nucl Med Mol Imaging.* 2015;42:197–209.

28. Hijazi S, Meller B, Leitsmann C, et al. Pelvic lymph node dissection for nodal oligometastatic prostate cancer detected by ^{68}Ga-PSMA-positron emission tomography/computerized tomography. *Prostate.* 2015;75:1934–1940.

29. Herlemann A, Wenter V, Kretschmer A, et al. ^{68}Ga-PSMA positron emission tomography/computed tomography provides accurate staging of lymph node regions prior to lymph node dissection in patients with prostate cancer. *Eur Urol.* 2016;70:553–557.

30. Chantadisai M, Buschner G, Kronke M, et al. Positive predictive value and correct detection rate of ^{18}F-rhPSMA-7 PET in biochemically recurrent prostate cancer validated by composite reference standard. *J Nucl Med.* 2020.

31. Langbein T, Kroenke M, Rauscher I, et al. Preliminary data on the diagnostic efficacy of F-18-rhPSMA-7.3 PET imaging for N-staging of patients with intermediate and high-risk prostate cancer compared to histopathology. Paper presented at: SNMMI, 2020. J Nucl Med. 2020;61(Suppl 1):1267.

32. Suardi N, Gandaglia G, Gallina A, et al. Long-term outcomes of salvage lymph node dissection for clinically recurrent prostate cancer: results of a single-institution series with a minimum follow-up of 5 years. *Eur Urol.* 2015;67:299–309.

33. Saigal CS, Gore JL, Krupski TL, et al. Androgen deprivation therapy increases cardiovascular morbidity in men with prostate cancer. *Cancer.* 2007;110:1493–1500.

34. Tsai HK, D'Amico AV, Sadetsky N, Chen MH, Carroll PR. Androgen deprivation therapy for localized prostate cancer and the risk of cardiovascular mortality. *J Natl Cancer Inst.* 2007;99:1516-1524.

Graphical Abstract

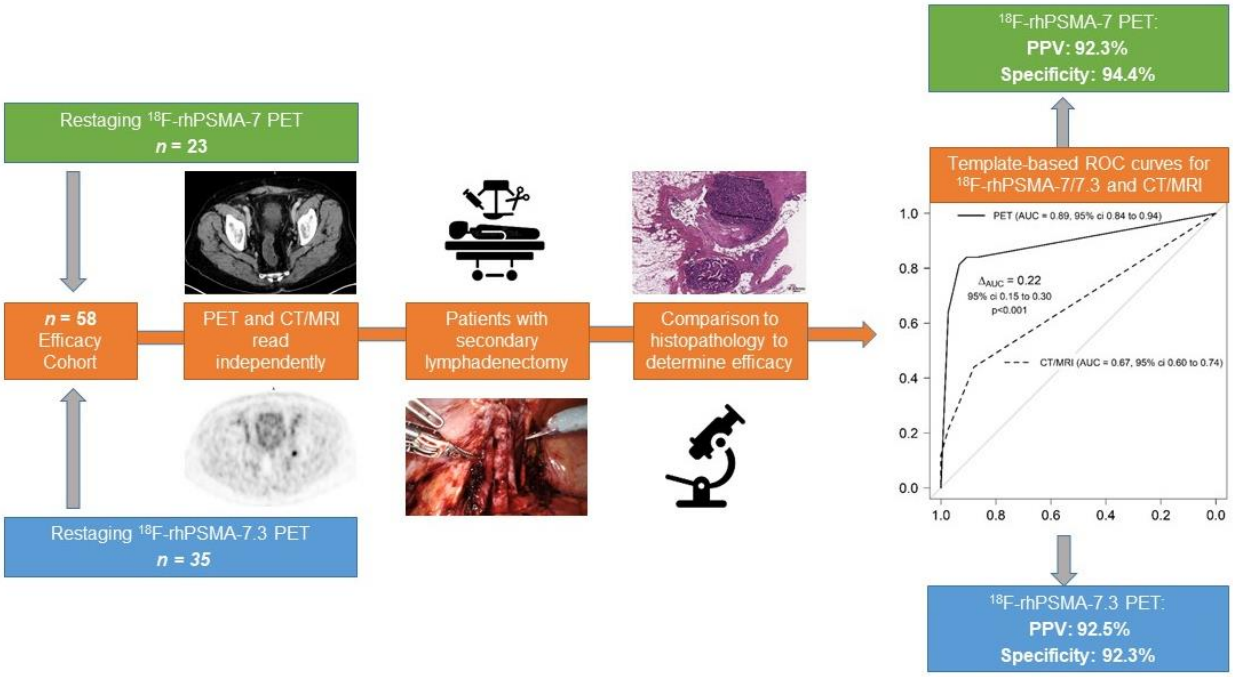

Figure 1 Template based ROC curves for combined data of ^{18}F-rhPSMA-7 and ^{18}F-rhPSMA-7.3 PET (black line) and morphological imaging (CT/MRI) (dotted line) for assessment of lymph node metastases in all 150 lymph node regions.

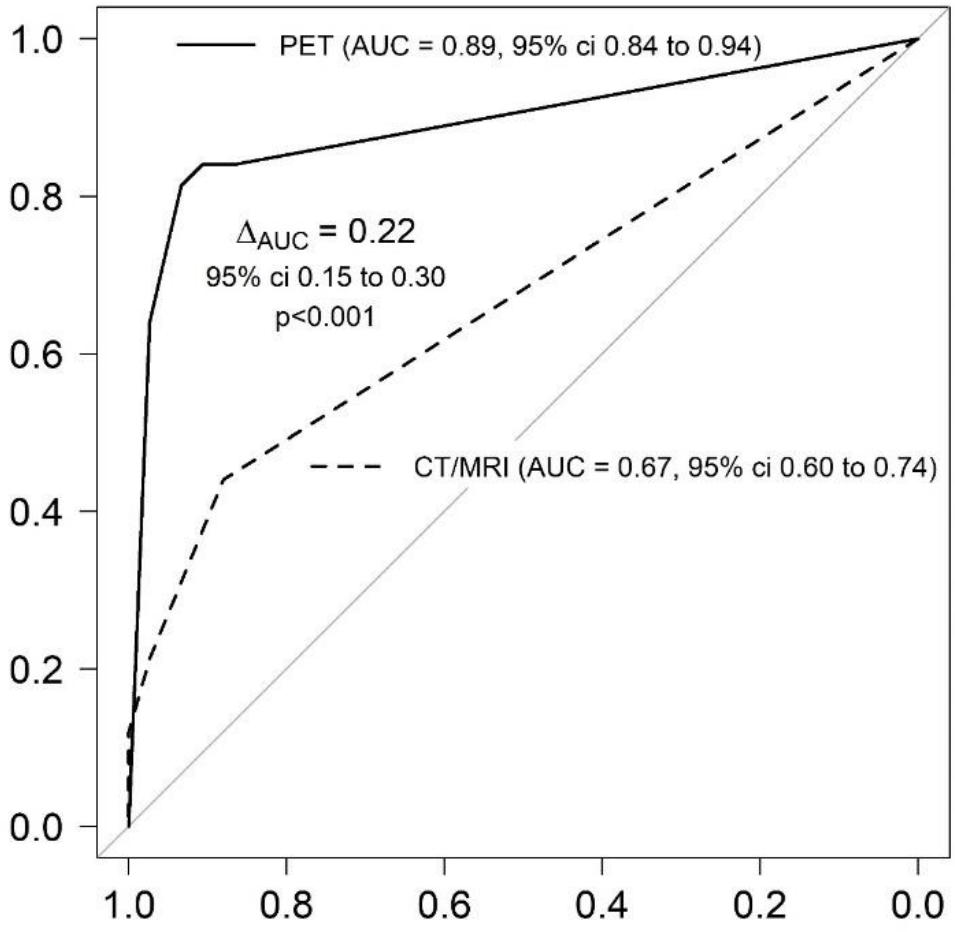

Figure 2

75-year-old patient with biochemical recurrence after radical prostatectomy (ISUP grade group 4, pT3b pN0 cM0, iPSA level: 11 ng/mL, PSA level at time of PET examination: 1.02 ng/mL) and a correctly classified lymph node metastasis by ^{18}F-rhPSMA-7.3 PET: a morphologically non-suspicious lymph node, 5 mm in diameter is visible in the left obturator fossa on CT (A and B) that shows intense, focal and suspicious tracer uptake in ^{18}F-rhPSMA-7.3 PET and fused PET/CT (C, E). Salvage lymphadenectomy with histologic evaluation confirmed a single lymph node metastasis (D, F).

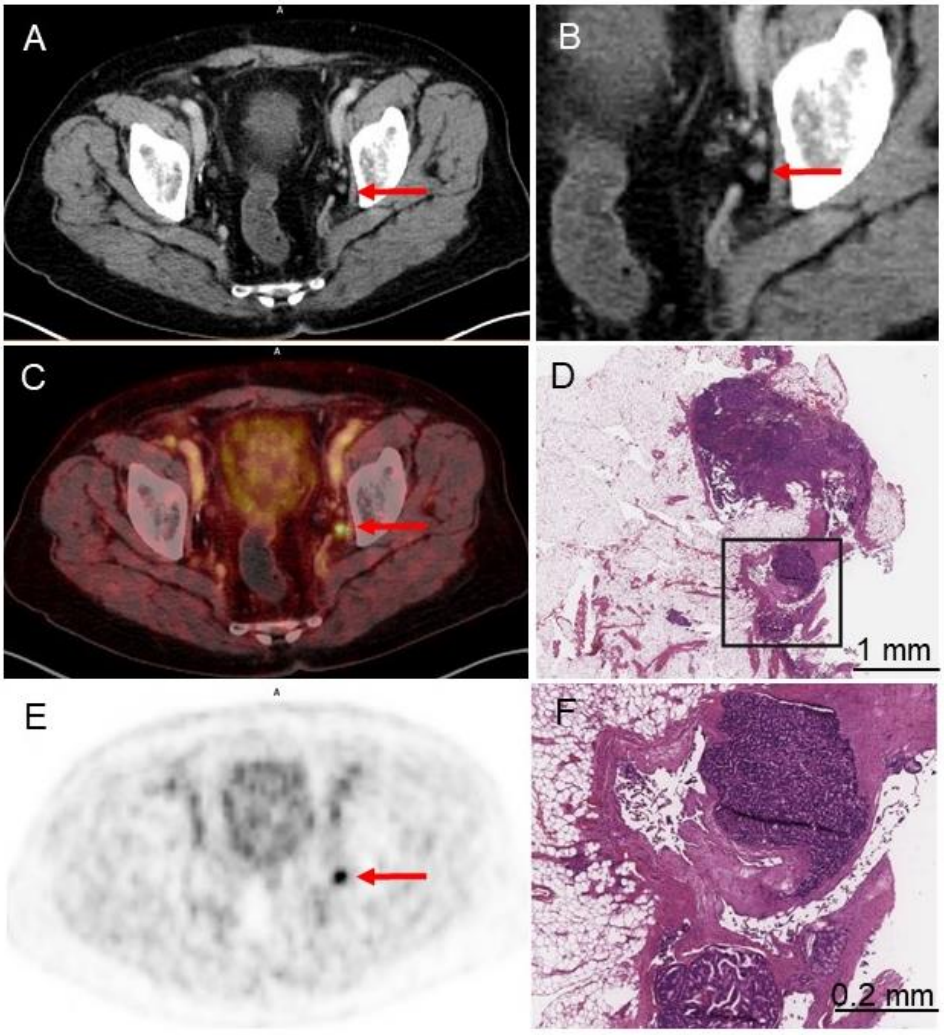

Table 1 Patient characteristics

N (%)	58 (100)
Age, y	
Median	68.5
Range	51-85
iPSA, ng/mL*	
Median	10.00
Range	1.9-57.9
ISUP grade, n (%)	
1-2	17 (29)
3-4	27 (47)
5	10 (17)
Missing	4 (6.9)
Pathological T-stage at primary RPE, n (%)	
≤pT2c	23 (40)
pT3a	11 (19)
≥pT3b	18 (31)
Missing	6 (10)
Pathological N-stage at primary RPE, n (%)	
pN0	39 (67)
pN1	10 (17)
Missing	9 (16)
Time between primary surgery and PET, months	
Median	48
Range	1-278
Pre-Scan PSA, ng/mL**	
Median	0.71
Range	0.16-8.39
Time between PET and salvage surgery, days	
Median	59
Range	19-117
Lymph node regions removed at salvage LAE	
N	150
Median	2
Range	1-9
Lymph nodes regions with metastases at salvage LAE	
N	75
Median	1
Range	0-4

*not available in 12 cases; **not available in one case.

iPSA, initial PSA concentration; ISUP, International Society of Urological Pathology; LAE, lymphadenectomy; PET, positron emission tomography; PSA, prostate specific antigen; RPE, radical prostatectomy.

Table 2 Template-based analysis

Combined data for ^{18}F-rhPSMA-7 and ^{18}F-rhPSMA-7.3	**Histology: lymph node metastasis**		
	Positive	**Negative**	
Positive	61	5	**PPV**: 92.4% (95% CI, 83.3-96.8%)
Negative	14	70	**NPV**: 83.3% (95% CI, 72.2-90.6%)
Total	75	75	150
	Sensitivity: 81.3% (95% CI, 70.1-89.0%)	**Specificity**: 93.3% (95% CI, 85.9-97.0%)	**Accuracy**: 87.3% (95% CI, 80.5-92.0)
Morphological Imaging (CT/MRI)	**Histology: lymph node metastasis**		
	Positive	**Negative**	
Positive	9	0	**PPV**: 100% (95% CI, n/a)
Negative	66	75	**NPV**: 53.2% (95% CI, 44.5-61.6%)
Total	75	75	150
	Sensitivity: 12.0% (95% CI, 6.3-21.6%)	**Specificity**: 100% (95% CI, n/a)	**Accuracy**: 64.5% (95% CI, 47.2-64.5%)

Scores ≥4 in PET and morphological imaging rated positive. NPV, negative predictive value; PPV, positive predictive value; n/a, not available as cannot be calculated (there exists no confidence interval for point estimator of 1 in GEE)

Supplemental Table 1 Patient data for those undergoing ^{18}F-rhPSMA-7 PET and subsequent salvage lymph node surgery

Pt	ISUP grade*, 1-5	pT*	pN*	Pre-scan PSA, ng/mL	Injected activity, MBq	PET modality used	No. regions resected	No. regions positive	PET assessment, 1-5	morphologic imaging assessment, 1-5
A1	5	3b	0	0.6	272	PET/CT	5	3		2
A2	4	—	—	0.25	348	PET/CT	4	1	5	4
A3	3	3b	0	0.4	266	PET/CT	3	1	5	2
A4	5	—	—	0.27	288	PET/CT	2	1	4	3
A5	3	2c	1	7.93	274	PET/CT	2	1	5	4
A6	3	3b	1	2.5	336	PET/CT	9	2	5	5
A7	2	2c	0	0.27	356	PET/CT	4	1	4	1
A8	5	3b	0	1.33	279	PET/MRI	1	1	5	1
A9	—	2c	0	1.18	344	PET/CT	2	2	5	5
A10	4	2a	0	1.05	362	PET/CT	5	1	5	4
A11	2	3a	0	0.66	239	PET/MRI	5	3	5	1
A12	3	2a	0	0.61	328	PET/MRI	1	1	5	1
A13	3	2c	0	0.97	346	PET/CT	2	1	4	1
A14	4	3a	1	0.32	399	PET/CT	1	1	5	1
A15	3	3b	1	0.35	270	PET/CT	2	1	5	2
A16	1	2c	0	0.76	303	PET/MRI	2	1	4	1
A17	2	—	—	0.41	340	PET/CT	3	0	4	2
A18	2	3a	0	0.21	272	PET/CT	1	1	5	3
A19	3	2c	—	0.83	300	PET/CT	3	1	5	2
A20	3	2a	0	0.26	308	PET/CT	2	0	1	1
A21	5	2c	1	0.21	258	PET/MRI	2	1	5	1
A22	—	—	—	6.13	328	PET/CT	1	1	4	1
A23	5	3a	0	0.24	344	PET/CT	4	1	5	3
									^{18}F-rhPSMA-7 PPV: 95.5%	

*Primary tumor

Supplemental Table 2 Patient data for those undergoing ^{18}F-rhPSMA-7.3 PET and subsequent salvage lymph node surgery

Pt	ISUP grade*, 1-5	pT*	pN*	Pre-scan PSA, ng/mL	Injected activity, MBq	PET modality used	No. regions resected	No. regions positive	PET assessment, 1-5	morphologic imaging assessment, 1-5
B1	2	2c	0	1.43	342	PET/CT	1	1	5	2
B2	4	3b	0	0.96	293	PET/CT	1	1	5	3
B3	4	3a	0	1.23	363	PET/CT	1	1	5	1
B4	4	3a	0	3.34	290	PET/CT	1	1	5	4
B5	2	3a	1	1.47	304	PET/MRI	1	1	5	4
B6	2	2c	1	4	341	PET/CT	1	0	4	2
B7	—	—	—	0.47	245	PET/CT	5	4	5	2
B8	3	2c	0	1.14	287	PET/CT	2	1	5	2
B9	2	3a	0	0.48	353	PET/CT	1	1	5	3
B10	2	3b	0	1.98	335	PET/MRI	2	1	5	2
B11	3	3b	—	0.29	338	PET/CT	4	1	4	2
B12	2	3b	0	0.43	303	PET/MRI	2	1	4	1
B13	4	2c	0	0.16	303	PET/CT	1	1	4	1
B14	3	3a	0	1.27	274	PET/CT	1	1	5	1
B15	1	2c	0	0.42	267	PET/CT	3	1	4	1
B16	2	2 c	0	0.16	385	PET/CT	1	0	4	1
B17	5	2c	0	1.12	379	PET/CT	4	2	5	1
B18	3	3b	0	0.6	317	PET/MRI	4	1	5	2
B19	5	3b	1	0.57	398	PET/CT	2	2	5	2
B20	2	3b	0	3	374	PET/MRI	1	1	5	3
B21	3	3b	—	0.82	311	PET/CT	4	3	5	2
B22	3	3a	0	0.8	396	PET/CT	4	2	5	2
B23	4	2c	0	0.42	298	PET/CT	1	1	5	3
B24	1	1c	0	4.4	311	PET/CT	4	2	5	5
B25	2	2c	0	1.06	358	PET/CT	1	1	5	1
B26	3	3b	0	1	326	PET/CT	3	3	4	2
B27	5	3b	0	1.05	322	PET/CT	2	1	5	5
B28	5	3b	0	0.43	376	PET/CT	4	1	5	2
B29	5	3	0	0.45	268	PET/CT	2	1	5	2

B30	2	2a	0	0.58	303	PET/CT	5	3	5	3
B31	3	2c	0	0.42	340	PET/CT	2	1	3	3
B32	3	2c	1	0.41	252	PET/CT	2	1	5	1
B33	—	—	—	8.39	280	PET/CT	3	3	5	1
B34	3	3b	1	0.8	338	PET/CT	4	1	4	3
B35	4	3b	0	1.02	340	PET/CT	4	1	5	2
										^{18}F-rhPSMA-7.3 PPV: 94.1%

*Primary tumor

Supplemental Table 3 Patient-based analysis

Rating ^{18}F-rhPSMA-7 and ^{18}F-rhPSMA-7.3 combined	**Histology: lymph node metastasis**		
	Positive	**Negative**	
Positive	53	3	**PPV**: 94.6% (95% CI, 85.1-98.9%)
Negative	1	1	**NPV**: 50.0% (95% CI, 1.3-98.7%)
Total	54	4	58
	Sensitivity: 98.1% (95% CI, 90.1-100%)	**Specificity**: 25.0% (95% CI, 0.6-80.6%)	**Accuracy**: 93.1% (95% CI, 83.3-98.1%)
Morphological Rating (CT/MRI)	**Histology: lymph node metastasis**		
	Positive	**Negative**	
Positive	9	0	**PPV**: 100.0% (95% CI, 64.4-100%)
Negative	45	4	**NPV**: 8.2% (95% CI, 2.3-19.6%)
Total	54	4	58
	Sensitivity: 16.7% (95% CI, 7.9-29.3%)	**Specificity**: 100.0% (95% CI, 39.8-100%)	**Accuracy**: 22.4% (95% CI, 12.5-35.3%)

Scores ≥4 in PET and morphological imaging rated positive. NPV, negative predictive value; PPV, positive predictive value

Supplemental Table 4 Template-based analysis for rhPSMA-7 and rhPSMA-7.3 separate

Rating ^{18}F-rhPSMA-7 only	Histology: lymph node metastasis		
	Positive	**Negative**	
Positive	24	2	**PPV**: 92.3% (95% CI, 75.6-97.9%)
Negative	2	34	**NPV**: 94.4% (95% CI, 71.2-99.2%)
Total	26	36	62
	Sensitivity: 92.3% (95% CI, 63.4-98.8%)	**Specificity**: 94.4% (95% CI, 84.2-98.2%)	**Accuracy**: 93.5% (95% CI, 83.2-97.7%)
Morphological Rating (CT/MRI)	**Histology: lymph node metastasis**		
	Positive	**Negative**	
Positive	5	0	**PPV**: 100% (95% CI, n/a)
Negative	21	36	**NPV**: 63.2% (95% CI, 49.3-75.1%)
Total	26	36	62
	Sensitivity: 19.2% (95% CI, 8.4-38.2%)	**Specificity**: 100% (95% CI, n/a)	**Accuracy**: 66.1% (95% CI, 52.1-77.8%)

Rating ^{18}F-rhPSMA-7.3 only	Histology: lymph node metastasis		
	Positive	**Negative**	
Positive	37	3	**PPV**: 92.5% (95% CI, 78.9-97.6%)
Negative	12	36	**NPV**: 75.0% (95% CI, 60.3-85.6%)
Total	49	39	88
	Sensitivity: 75.5% (95% CI, 62.2-85.2%)	**Specificity**: 92.3% (95% CI, 78.8-97.5%)	**Accuracy**: 83.0% (95% CI, 73.2-89.7%)
Morphological Rating (CT/MRI)	**Histology: lymph node metastasis**		
	Positive	**Negative**	
Positive	4	**0**	**PPV**: 100% (95% CI, n/a)
Negative	**45**	39	**NPV**: 46.4% (95% CI, 36.6-56.5%)
Total	48	36	84
	Sensitivity: 8.2% (95% CI, 3.0-20.1%)	**Specificity**: 100% (95% CI, n/a)	**Accuracy**: 48.9% (95% CI, 38.9-58.9%)

Scores ≥4 in PET and morphological imaging rated positive. NPV, negative predictive value; PPV, positive predictive value; n/a, not available as cannot be calculated (there exists no confidence interval for point estimator of 1 in GEE)